Isı Bilimi ve Tekniği Dergisi, 38, 2, 63-74, 2018
J. of Thermal Science and Technology

ISSN 1300-3615

# EXPERIMENTAL INVESTIGATION OF HEAT TRANSFER WITH A TRANSVERSELY PULSATING JET ON A FLAT PLATE

**Ünal AKDAĞ* , Selma AKÇAY**, Doğan DEMİRAL* and Hakan PALANCIOĞLU***
* Aksaray University, Department of Mechanical Engineering
68100 Aksaray, uakdag@gmail.com
** Aksaray University, Institute of Science and Technology
68100 Aksaray, selma.352@hotmail.com

(Geliş Tarihi: 23.05.2017, Kabul Tarihi: 17.07.2018)

**Abstract**: In this study, the effect of a transversely pulsating jet on heat transfer over a flat plate is investigated experimentally. The experimental study consists of a heater and a pulsating jet. The heater is made of a copper plate, has a constant heat flux, and is located in a wind tunnel. The pulsating jet is injected into the stream at the plate entrance. The pulsating jet is created using an oscillating movement of a piston-cylinder mechanism, and the secondary mass flux is supplied using a high-pressure blower. In the study, the Reynolds number in the main stream, the pulsating jet frequency and amplitude are changed, while the geometry and the other parameters remain constant for all cases. Furthermore, the effect of these parameters on heat transfer is analyzed. The experiments are performed for four different amplitudes and six different frequencies at four different blowing ratios. To explain the heat transfer mechanism, flow visualization is performed using the smoke–wire method, and instantaneous flow images are obtained. It is observed that, the surface cooling performance increases with the increase of both the pulsating frequency and amplitude at high blowing ratios. The calculated experimental results are given as a function of dimensionless parameters.
**Keywords:** Pulsating jet, Flat plate, Heat transfer enhancement, Film cooling.

# DÜZ BİR LEVHA ÜZERİNDE ENİNE PULSATİF BİR JET İLE ISI TRANSFERİNİN DENEYSEL İNCELENMESİ

**Özet:** Bu çalışmada, düz bir levha üzerinde ısı transferine enine pulsatif bir jetin etkisi deneysel olarak incelenmiştir. Deneysel çalışma bir ısıtıcı ve pulsatif bir jetten oluşmaktadır. Isıtıcı, sabit ısı akısına sahip bakır bir levhadan yapılmış ve rüzgar tünelinin içine yerleştirilmiştir. Pulsatif jet, levha girişinde akış içerisine enjekte edilmektedir. Pulsatif jet, piston-silindir mekanizmasının salınım hareketi ile oluşturulmakta ve ikincil kütle akısı yüksek basınçlı bir fan kullanılarak sağlanmaktadır. Çalışmada, ana akış Reynolds sayısı, pulsatif jet frekansı ve genliği değiştirilirken geometri ve diğer parametreler tüm durumlar için sabit kalmaktadır. Ayrıca, ısı transferi üzerinde bu parametrelerin etkisi analiz edilmektedir. Deneyler, dört farklı genlik, altı farklı frekans ve dört farklı üfleme oranı için gerçekleştirilmiştir. Isı transferi mekanizmasını açıklamak için duman-tel metodu ile akış görüntüleme yapılmış ve anlık akış görüntüleri elde edilmiştir. Yüksek üfleme oranlarında, pulsatif frekans ve genliğin her ikisinin de artması ile yüzey soğutma performansının arttığı gözlemlenmiştir. Elde edilen deneysel sonuçlar boyutsuz parametrelerin bir fonksiyonu olarak verilmiştir.
**Anahtar kelimeler**: Pulsatif jet, Düz levha, Isı transferi iyileştirme, Film soğutma

## NOMENCLATURE

| | |
|---|---|
| $A_o$ | dimensionless amplitude |
| $d$ | blower nozzle of the actuator [m] |
| $h(x,t)$ | local-instantaneous heat transfer coefficient [W/m$^2$K] |
| $k$ | thermal conductivity [W/m.K] |
| $L$ | heater plate length [m] |
| $L_t$ | total model length [m] |
| $M$ | blowing ratio |
| $Nu_{x,t}$ | local-instantaneous Nusselt number |
| $Nu_p$ | cycle average Nusselt number |
| $q''$ | heat flux [W/m$^2$] |
| $Pr$ | Prandtl number [=μCp/k] |
| $Re$ | Reynolds number [=$U_\infty L_t/\upsilon$] |
| $St$ | Strouhal number [=$fL/U$] |
| $x_m$ | amplitude (piston stroke) [m] |
| $x_o$ | unheated starting length [m] |
| $\overline{T}_w$ | cycle-average wall temperature [°C] |
| $T_\infty$ | forced flow-average fluid temperature [°C] |
| $U_\infty$ | forced flow inlet velocity [m/s] |
| $U_j$ | jet blowing velocity [m/s] |

*Wo* Womersley number

**Greek symbols**

$\rho$ fluid density
$\eta$ enhancement factor
$\omega$ angular frequency [rad/s]
$\tau$ cycle time [=$\omega$t]
$\upsilon$ kinematic viscosity [$m^2$/s]

## INTRODUCTION

The performance of devices used in the industrial, aerospace, power generation and electronic industries as well as of various engineering applications increases daily. In addition the power requirements of main components that are used in these systems also increases. As a result, the increasing power requirement causes overheating of working parts. The excessive rise in temperature causes mechanical strength weakening of metals parts, deterioration, over-expansion and poor performance of the system, which causes a decrease in the system lifetime. Therefore, recently, effective cooling of the heated parts in many engineering applications has attracted significant attention as a research topic. Heat transfer with forced convection on a flat plate has been commonly used as a cooling system for overheating components. Unfortunately, forced convection alone is insufficient to remove the overheating problem. Therefore, to ensure the effective heat transfer of film cooling, impingement jet, and periodic flow cooling are current research topics as alternative cooling methods**.** In the past decade, heat and mass transfer with pulsating jet or periodic fluctuation on the target surface have attracted a considerable scientific attention.

Film cooling is among the techniques commonly used to protect overheating surfaces. In film cooling, cool air is discharged from rows of holes to form a thin film on the surface. A protective air layer is covered between the surface and mainstream so, the heat can be removed from the surface more quickly. Experimental and numerical studies have shown that film cooling effectiveness is influenced by several parameters (e.g., discharge geometry, ejection angle, blowing ratio, surface geometry, density and temperature ratio) (Koc *et al*, 2009; Sidik *et al*, 2013; Audier *et al*, 2016; Wu *et al*, 2016; Schreivogel *et al*, 2016), and reliable prediction methods are needed to optimize the design. The application of film cooling has been studied extensively, both numerically (Kanani *et al*, 2008; Lee and Kim, 2014; Xie *et al*, 2015) and experimentally (Engels *et al*, 2001; Elnady *et al*, 2013; Liu *et al*, 2013; Ramesh *et al*, 2016). An experimental study was performed on film cooling performance of laterally inclined diffuser-shaped cooling holes by Heneka *et al* (2012). The results clearly showed the influence of cooling holes geometry on a flat plate using infrared thermography. Therefore, it was reported that an increase in the area ratio and compound angle, usually caused higher values of effectiveness. Singh *et al* (2016), presented an experimental study to examine film-cooling on a flat surface from the short cylindrical blowing holes the length-to-diameter (*L/D*) in the range 1–2, for five injection angles, five mainstream Reynolds numbers ($Re$=1.25 × $10^5$ –6.25 × $10^5$ ) and two blowing ratios ($M$ = 0.5 and $M$=1.0). The results shown that film-cooling performance was effected from the length of the holes and better performance was obtained at the lowest tested injection angle ($\alpha$ = 15°) in the near hole region. Dai *et al* (2016), numerically analyzed film cooling effectiveness from a cylindrical hole with parallel auxiliary holes influences for four blowing ratios, and they reported that the auxiliary holes improved film-cooling effectiveness. Tu *et al* (2017), numerically investigated the film cooling effectiveness using single row of round holes on a flat plate for various angles of inclination in two different directions as the axial angle $\alpha$ and the spanwise angle $\beta$ with anisotropic thermal conductivity. The numerical results denoted that the cooling effectiveness was affected from the inclined angles of the holes and the blowing ratios.

Pulsations have an important effect on the film cooling performance. A higher cooling effectiveness can be achieved when pulsating flow with film cooling is used. Periodic fluctuations caused by pulsating flow on the surface are increased the heat and mass transfer. It has many important applications, such as cooling of electronic components and drying of paper and glass. Recently, there has been an increase in the number of numerical studies about pulsating flow (Marzouk *et al*, 2015; Erkoc *et al*, 2016). The effect of pulsation on film cooling with a row of compound angle film cooling holes experimentally was studied by Lee and Jung (2002), and the adiabatic film cooling effectiveness distributions were measured using the Thermo-chromic Liquid Crystal (TLC) thermography. In their study, the orientation angles of 0º, 30º, 60º, 90º were considered at a fixed inclination angle of 35º. The results showed that the film cooling effectiveness reduced at all orientation angles, and was better at smaller blowing ratios. Coulthard *et al* (2007) experimentally investigated the pulsed film cooling effectiveness for a single row of cylindrical film-cooling holes inclined at 35 degrees on a flat plate at different blowing ratios. They reported that higher pulsing frequencies enhanced the film-cooling effectiveness. However, at lower frequencies, pulsing did not provide any overall benefit, and the highest effectiveness was obtained with steady jets and a blowing ratio of 0.5. Sultan *et al* (2016), experimentally studied the effects of film cooling with using sinusoidal pulsations to an oblique round jet for different the blowing ratios and different Strouhal number. It was reported that in blowing ratio of $M$= 1.25, film-cooling effectiveness increased significantly at low-frequency pulsation during a pulse cycle.

Because of the flow structures complexity and non-linear dynamics in the boundary layer induced by pulsation, the pulsed transverse jet flow and the associated heat transfer

have been challenging problems and showed some intriguing aspects. The related pulsating flowphysics is not yet well-understood (Li *et al*, 2013). Therefore, in this study, the effect of a transversely pulsating jet on the heat transfer over a flat plate was investigated experimentally. A secondary mass flux was injected into the main stream using a transversely pulsating jet at the entrance of a flat plate. This is a type of film cooling problem. The effect of physical parameters has been analyzed to further the understanding of flow and thermal characteristics in the pulsed blowing film cooling. In the previous studies, single or multiple hole geometries were used in different diameters and shapes on the plate and the secondary mass flux was blown from the holes with different arrays. For this reason, it is inevitable that there will be some temperature difference in the region between the holes. In this study, a transverse pulsating jet was used differently than the other previous studies. The secondary mass flux is blown from a longitudinal channel located at the front of the plate, not the holes. As the second fluid completely covers the surface of the plate, no temperature difference will occur on the surface of the plate.

## EXPERIMENTAL STUDY

### Experimental Setup

Fig.1. shows the schematic view of experimental setup used in this study. An Eiffel type open wind tunnel (Gunt HM-170) was used to perform the experiments. The tunnel test section dimensions are 300×300×450 mm with a maximum velocity of 28 m/s. The experimental set-up was described in detail in previous papers (Akdag *et al*, 2013; Akdag *et al*, 2016; Akdag *et al*, 2017). In Ref (Akdag *et al*, 2013), the effect of a synthetic jet on the heat transfer of flow over a flat plate was investigated experimentally. Where, the synthetic jet was defined as "zero-net-mass-flux" jet. In present study, the pulsating jet was used and included the secondary mass flux jet different than synthetic jet. So, unlike pulsating jet synthetic jet, it contains an additional mass flux. The previous setup was arranged and using additional devices, the design was converted into a pulsating jet experimental setup. In the setup, air enters into the wind tunnel through a bell mouth of the settling chamber, that contains a honeycomb (to reduce swirling) and a set of screens (to obtain a uniform velocity). It was driven by a speed-controlled motor with a frequency converter. A test model was placed in the middle of the test section including the pulsating jet actuator.

The experimental test model was constructed from four different parts, and the final dimensions are 260 × 212 × 32 mm. The heater platform consisted of four parts (i.e., a 2 mm copper plate, a 1 mm Kapton heater, a 15 mm rock-wool insulation and a 6 mm Plexiglas jet channel section). These four parts were combined together with a specially constructed wooden frame, as shown in Fig. 2. The heater model, which was located in the middle of the test section, has a smooth surface finish. Additionally, $x$ is the stream-wise direction, $y$ is normal to the flat plate, and $z$ is lateral to the flat plate. The leading edge of the experimental model has an angle of $\theta$=30° to avoid boundary layer separation. The heater module is made using a copper plate and a thin Kapton heater. The flexible Kapton heater (Omega, KHR flexible) is used to provide a constant heat flux output ($q''$=762 W/m$^2$) and is affixed to the bottom surface of the copper plate. It is assumed that there is a uniform heat flux the entire plate surface.

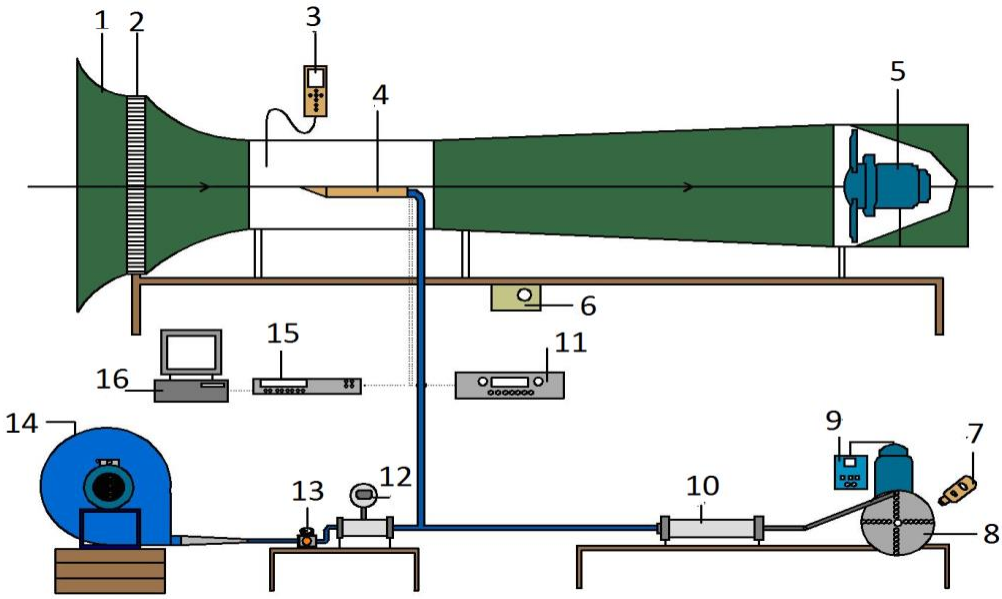


**Fig. 1.** Experimental Setup *(1. Nozzle, 2. Honeycomb, 3. Hot-wire probe, 4. Experimental model, 5. Axial fan, 6. Motor controller, 7. Digital tachometer, 8. Flywheel, 9. DC-Motor and control unit, 10. Piston–cylinder apparatus, 11. Power supply, 12. Flowmeter, 13. Pressure regulator, 14. Radial fan, 15. Data acquisition system, 16. CPU)*

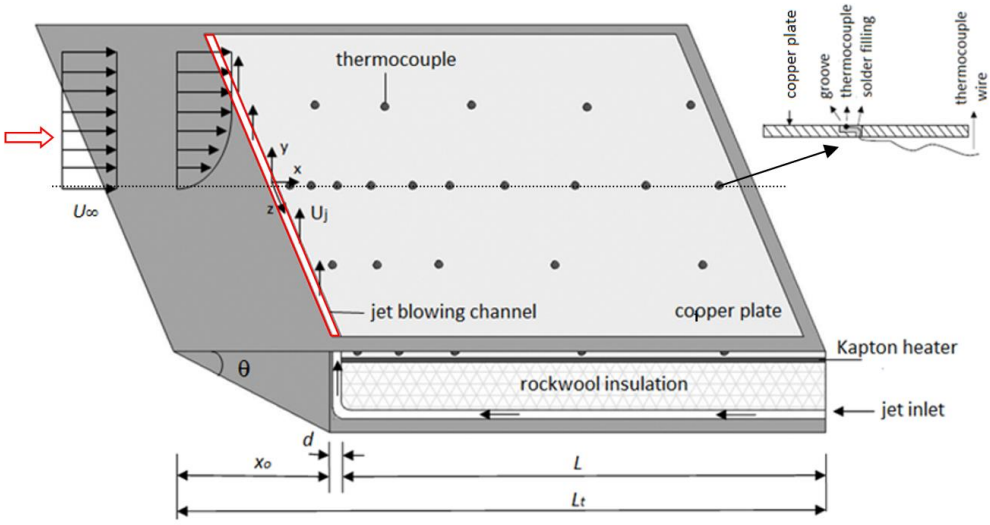


**Fig.2** Geometry of the experimental test model

The heater module is insulated with rock-wool to minimize the heat loss through the bottom and to allow heat transmission from the heater to the copper plate. It is assumed that the power input to the heater equals the total output of the heat transfer from the heater surface. The heater plate dimensions are 200 × 200 mm. The pulsating jet actuator is flush mounted on the test surface. The jet actuator has a $d$=3 mm blower nozzle and is transversely located at the heater entrance with 90 degree angle. This angle is chosen to provide the maximum interaction between the pulsating jet and the free stream. The jet movement is created using a piston-cylinder mechanism driven by a powerful DC motor (2.2 kW) with an adjustable speed and used a high-pressure blower. The blower (EN60335; 5.5kW, 9000Pa, 1200m$^3$/h) produces a secondary mass flux and is controlled by a pressure regulator. The secondary mass flux is fixed at a constant flowrate as 10 m$^3$/h for all experiments, and it is measured using a swirl type flowmeter (ABB FS4000, ±0.05 m$^3$/h). A flywheel was used to adjust the pulsating jet amplitude movement. The number of motor revolutions is measured by an optical digital tachometer. Air is used as a working fluid in the present experiments.

**Experimental Measurements**

Experimental results are obtained based on the temperature measurements. The temperature measurements are performed on the plate surface according to the operating parameters for the calculation of heat transfer. Thermocouples were used for this purpose, and they were specifically located in the experimental system. Thermocouples are soldered to the copper plate surface in the specially created grooves. Roughness is removed from the soldered points to maintain a smooth surface, to minimize disturbances in the flow. The structure of heater and welded thermocouple locations are shown in Fig.2. For the temperature measurements, a high measurement speed data acquisition system (Keithley-2750, sample: 2500 readings/s) was employed that was coupled with K-type (Omega, ±0.1°C) thermocouples. In total, twenty-two thermocouples were used in the setup. Two identical thermocouples were used away from the heater surface to measure the ambient air temperature ($T_\infty$) in the wind tunnel. The remaining twenty thermocouples were located on the copper plate to measure the surface temperature. The thermocouple cables were placed between the Kapton heater and the copper plate and were passed through the back of the model to be connected to the data acquisition system. Ten thermocouples were located at inline positions along the plate to give an average representative value of the heater surface temperature ($T_w$). The other ten thermocouples are used to control the surface temperature measurement. The positions used for the thermocouples are shown in Fig.3.

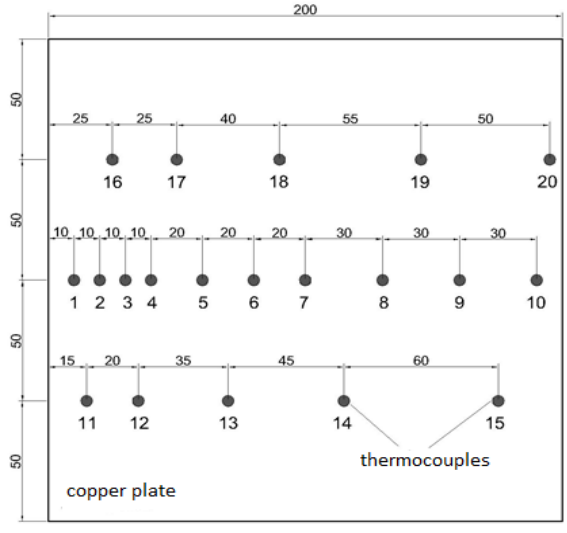

**Fig.3.** Thermocouple positions on the copper plate surface

In Fig. 4 is shown that there is no difference between the temperature measured by the thermocouples in the center and the edge of plate. Because of low surface temperature, heat loss from the surface due to radiation transfer is neglected, as it is calculated to be less than 1% of the power input. The heater surface is made of a thin-walled copper plate. The calculated Biot number is very small ($Bi$=0.0002) and the plate is assumed lumped (Incropera and DeWitt, 2002). Thus, the effect of the heat conduction along the wall can be neglected.

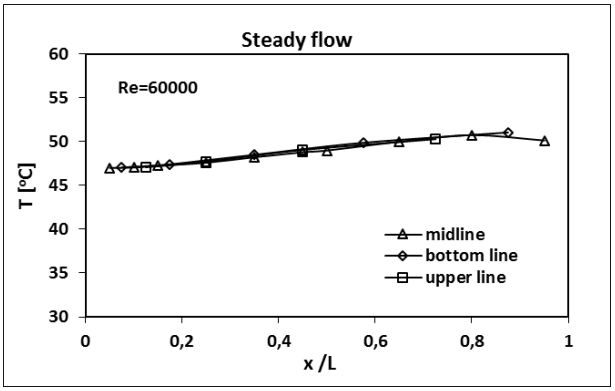


**Fig. 4.** Temperature distribution according to thermocouple positions on the copper plate surface

In the wind tunnel, velocity measurements have been conducted under ambient conditions using a single hotwire anemometer (Testo-435, ±0.2 m/s). The average velocity is set at a fixed value to ensure the intended Reynolds number. First, the Reynolds numbers are changed, and the temperature measurements are recorded at steady flow conditions. Then, the Nusselt numbers are calculated and compared with the literature (Incropera and DeWitt, 2002) to ensure the accuracy of temperature measurements over the plate surface in the laminar boundary layer. The comparison of the results is given in Fig.5. This comparison showed that the experimental and theoretical results (Eqn.1) were in good agreement for the steady flow conditions.

$$Nu_m = \frac{h_m L_t}{k} = 0,662 \frac{[1-(x_o / L_t)^{3/4}]^{2/3}}{L_t - x_o} Re_x^{1/2} Pr^{1/3} \quad (1)$$

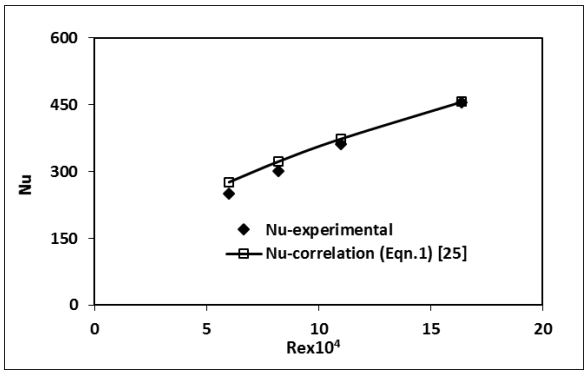


**Fig. 5.** The comparison of experimental results with literature (Incropera and DeWitt, 2002)

Secondly, radial fan is activated, and the second mass flux is continuously injected into the main flow from the blowing channel. The pulsating jet flowrate is fixed for the experiments. The temperature measurements are recorded for the continuous jet flow conditions. Then, the Nusselt numbers are calculated. The blowing ratio is determined as $M=\rho_j U_j/\rho_\infty U_\infty$. Different blowing ratios are obtained by changing the main stream velocity. The jet velocity was kept constant for all cases (The Reynolds number and blowing ratio are dependent parameters). Finally, the pulsations are activated. Then, temperature measurements are recorded for the pulsating jet conditions, and the Nusselt numbers are calculated.

These experiments are performed for six different pulsating frequencies and for four different amplitudes. The experiments are repeated to examine the effect of blowing ratio at four different blowing ratios. Due to focus on the heat transfer enhancement, detailed velocity profiles and discussion of fluid dynamics of the periodically actuated flows are not presented. Experimental parameters are determined by taking into account the experimental setup limitations (Akcay, 2015). In this study, 96 experiments were performed.

**Experimental Uncertainties**

The uncertainty in the experimental data can be considered by identifying the main sources of errors in the measurements. The main source of errors in the reported results of the Nusselt numbers are the statistical uncertainties caused by the measurements of forced flow velocity ($U_\infty$, ±0.5 m/s), jet velocity ($U_j$, ±0.2 m/s) heater surface temperatures ($T_w$, ±1 °C) and free stream fluid temperature ($T_\infty$,±0.2°C). The uncertainty of the Nu numbers for each experiment is calculated by Equation (2). The total uncertainty of the Nu number is obtained with the arithmetic mean of the uncertainties in all experiments. More detailed information is available in Reference (Kline and McClintock, 1953).

$$w_{Nu} = \left[ \left( \frac{\partial Nu}{\partial T_w} w_{T_w} \right)^2 + \left( \frac{\partial Nu}{\partial T_\infty} w_{T_\infty} \right)^2 + \left( \frac{\partial Nu}{\partial U_\infty} w_{U_\infty} \right)^2 + \left( \frac{\partial Nu}{\partial U_j} w_{U_j} \right)^2 \right]^{1/2} \quad (2)$$

The averaged uncertainty value of the Nusselt numbers was computed to be approximately ±6.93% for the pulsating jet on the flat plate using the uncertainty estimation method described by Kline and McClintock (1953).

**Dimensionless parameters**

For present study, one-dimensional (only in x direction) analysis is performed depending on the physical parameters. Four dimensionless parameters are obtained to describe present problem. These parameters are the main stream Reynolds number (*Re*), blowing ratio (*M*), dimensionless amplitude ($A_o$) and the dimensionless frequency Womersley number (*Wo*). These parameters are defined as;

$$Re = \frac{U_\infty L_t}{\upsilon} \tag{3}$$

$$M = \frac{\left(\rho_j U_j\right)}{\left(\rho_\infty U_\infty\right)} \tag{4}$$

$$Wo = L/2\sqrt{\frac{\omega}{\nu}} \tag{5}$$

$$A_0 = \frac{x_m}{L} \tag{6}$$

where $U_\infty$ denotes the free stream (i.e., forced flow) mean velocity, $U_j$ is the jet blowing velocity, $L_t$ is the total plate length, $L$ is the heated plate length (the characteristic length), ω is the angular frequency, $x_m$ is the amplitude (piston stroke), and υ is the air kinematic viscosity. Because the Womersley number doesn't depend on the flow velocity and is more suitable for low frequencies, the dimensionless frequency is presented with *Wo* number in present study (Rohlf and Tenti, 2001; Loudon and Tordesillas, 1998). The experimental results for the heat transfer are presented in terms of the Nusselt number in detail in the next section.

**RESULTS and DISCUSSION**

In this section, the heat transfer mechanism is discussed using the pulsating jet on the heated flat plate by examining the effects of various parameters. The jet velocity, the Prandtl number (*Pr*=0.71) and geometric parameters are kept constant for all cases. Four different blowing ratios between the jet and free stream are used, specifically, *M=0.5, M=0.75, M=1, M=1.35*. In this study, the pulsations formed a time-dependent periodic flow field on the plate, so heat transfer was obtained periodically. Therefore, the heat transfer calculations are performed according to the amount of heat transfer obtained during one pulsating cycle. This means that the flow changes depending on time-periodically. To explain how the mechanisms behave over a cycle, phase angles have been used and are denoted by (ωt). The $\tau$ =360 degree indicates one cycle. First, the initial transient conditions are discarded and the results are analyzed after the variables reach a periodic behavior. The main parameters are the blowing ratio (Reynolds number), amplitude ($A_o$) and frequency (*Wo*), and the affected heat transfer characteristics of the periodic flow field.

In this study, for the heat transfer calculation, detailed temperature measurements are performed. The variation of time-averaged surface temperatures along the plate due to amplitude and frequency are shown in Fig.6. Local surface temperatures are calculated by averaging the instantaneous temperatures that are measured on the heated plate surface. $T_{w,x}$ is local temperatures were calculated as follows;

$$T_{w,x} = \frac{1}{N\Delta t}\sum_{i=1}^{N} T_{w,i}(x,t)\Delta t \tag{7}$$

where $N$ is the total number of data, $\Delta t$ is the time interval, and $T_{w,i}$ is the instantaneous measured temperatures. Time-averaged surface temperatures are calculated by averaging the local temperatures that are measured on the heated plate surface (Eqn.8).

$$\bar{T}_w = \frac{T_1 + T_2 + T_3 + T_4 + T_5 + T_6 + T_7 + T_8 + T_9 + T_{10}}{10} \tag{8}$$

To compare the surface cooling effect, the steady flow (no jet) and continuous jet conditions are presented together with the pulsating jet results in these figures. Where, *Wo* = 0 and *Wo*=1 represent steady flow and continuous jet flow, respectively. When comparing the pulsating jet conditions with the steady flow and continuous jet conditions, the pulsating jet provides better performance for the cooling of hot surface. It is evident that surface temperatures are lower for the pulsating jet compared with all other cases (Fig. 6). Surface temperatures change due to frequency and amplitude. Surface temperature decreases with the frequency increase. This means that, heat transfer increases with the increase in frequency at higher amplitudes. When the amplitude is low, surface temperatures are very close to each other. When the amplitude increases, the difference in surface temperatures increases with increasing frequency. At higher amplitude, the frequency effect significantly increases, which enhances the heat transfer.

Amplitude significantly affects the enhancement in heat transfer due to the increase in convective effect or interaction of fluid mixing between the forced flow and pulsating jet. The extent of interaction between the pulsating jet and laminar boundary layer depends on the strength of generated vortices and their transport capacity over the surface. It is obvious that pulsating jet increases the cooling performance of hot surfaces. This information is revealed in the temperature data as well as in the flow images.

**Flow visualization**

For the analysis of flow structure on the flow field, flow visualization experiments were performed using the smoke–wire method in the wind tunnel. Visualization photographs are obtained with a higher resolution color camera. The camera had a relatively long exposure to capture the instantaneous flow structure for the flow of *Re*=60000. Smoke–wire was made from three resistance wires (0.2 mm in diameter each), that were uniformly twisted together. The resulting smoke-wire was coated with paraffin oil before each test and was heated using a DC power supply. A light bulb was used as a light source. The time mean flow field patterns were obtained.

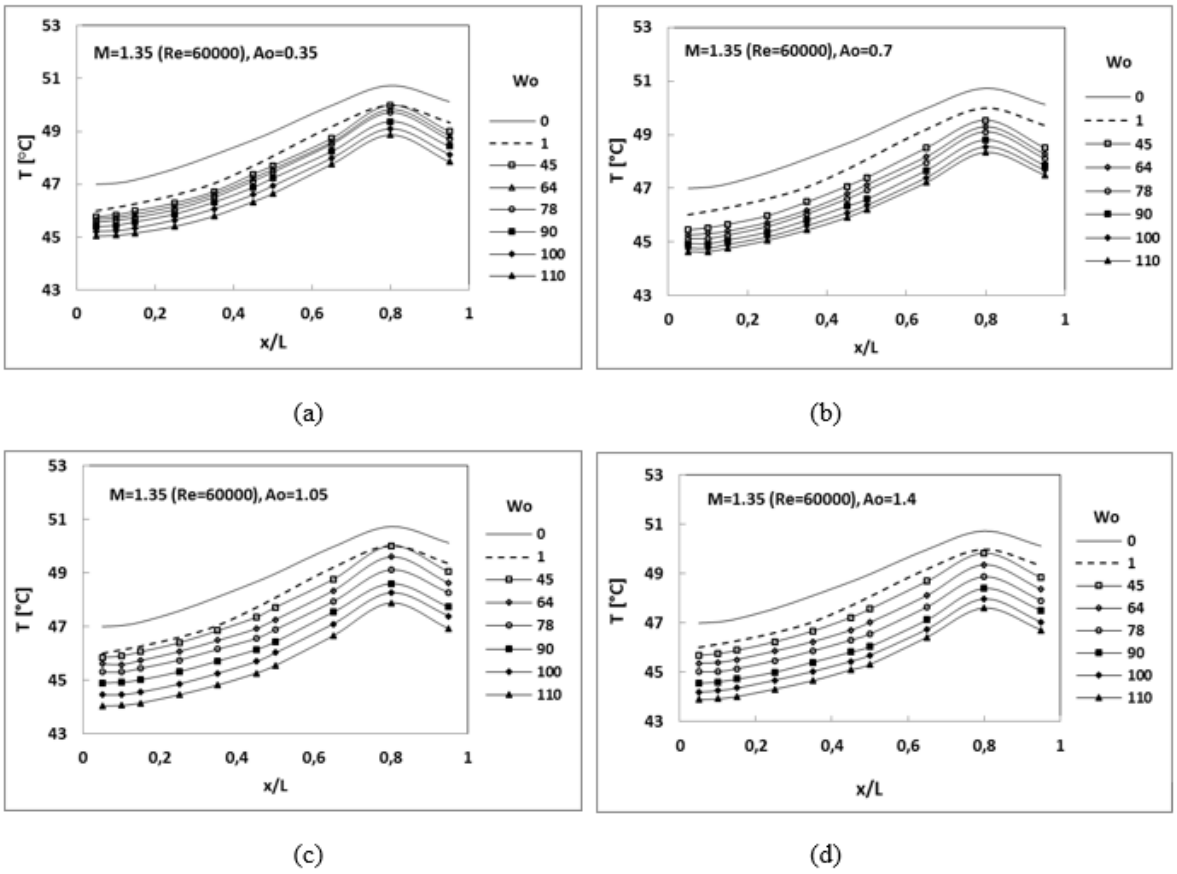


**Fig. 6.**Temperature variation along the plate versus the amplitude and frequency, (*Wo*=0: steady flow, *Wo*=1: continuous jet)

The variations of flow structure on the plate produced by injecting pulsating jet are illustrated in Fig.7a and 7b. The flow visualization results for a constant frequency (*Wo*=110) and different amplitudes with a phase angle of 270° are shown in Fig.7a together with a steady flow. For a steady flow, the fluid flow in the boundary layer is very regular, and the streamlines are parallel to the plate. For pulsating jet, the flow field is changed along the plate by jet actuation with an increase in amplitude compared with a steady flow. Due to the pulsating jet causes mass and momentum transfer, the boundary layer is lifted-off on the plate. The temperature and flow field are changed along the plate. The pulsations cause fluctuation effect on the plate surface, which provides good mixing in the flow field along the plate. For the higher amplitude ($A_o$=1.4), a strong lift-off region is observed in the time-averaged flow field at a higher frequency. There was a disruptive effect on the hydrodynamic boundary layer of flow pulsations. The changes in flow hydrodynamics are effects the thermal boundary layer, and hot fluid layer on plate propagates into the free stream region. It leads to heat transfer enhanced. Consequently, pulsating jet affects to the flow field and heat transfer regime, and contributes to the improvement in heat transfer.

Fig.7b presents the flow pattern images over a cycle for the specific amplitude ($A_o$=1.4) and frequency (*Wo*=110). To better understand the mechanisms that lead to the improved cooling effect of surface with a pulsating jet, a sequence of instantaneous images is presented over the cycle. The pulsating jet changes flow structures using the momentum and mass transfer. The flow structure in the boundary layer is changed for every phase angle during the pulsating cycle. It causes big fluctuation due to the interaction of forced flow at the leading edge of the plate.

Because the flow is time periodic, the fluctuations are achieved periodically in the flow field, thus, the temperature field varies with time over a cycle. As shown in the figure, the flow structures are changes significantly

by jet blowing. Because of the periodicity, the fluid in the boundary layer is dispersed into the free stream region over a cycle. It is concluded that the heat transfer is significantly affected by the pulsating jet actuator, and amplitude has the dominant effect. The role played by the amplitude in enhancing heat transfer is clearly demonstrated by flow visualization and is further confirmed by temperature measurements.

**Calculation of the Nusselt number**

To calculate heat transfer for the steady flow, such as a flat plate ($Nu_s=h_sL/k$), the local instantaneous Nusselt number along the flat plate can be expressed as follows:

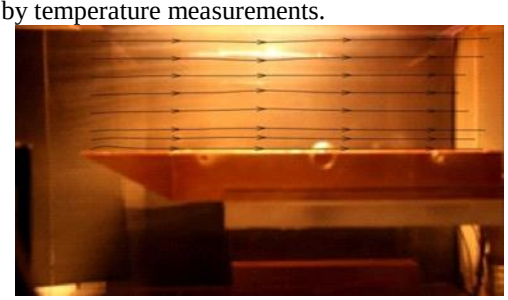

*steady flow*

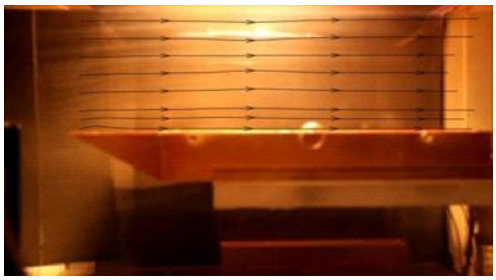

*steady flow*

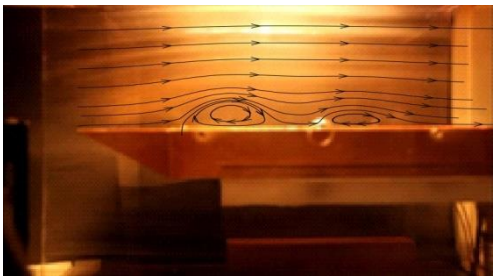

$A_o$=0.35, *Wo*=110, ωt=3π/2

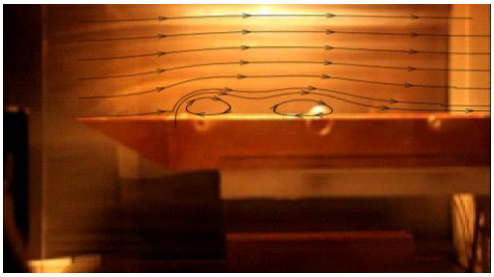

$A_o$=1.4, *Wo*=110, ωt=0

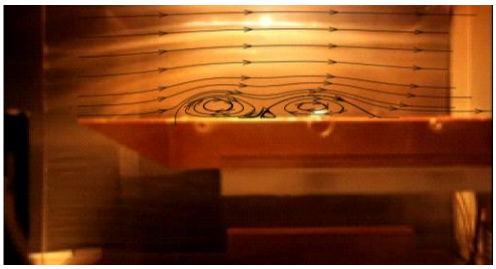

$A_o$=0.7, *Wo*=110, ωt=3π/2

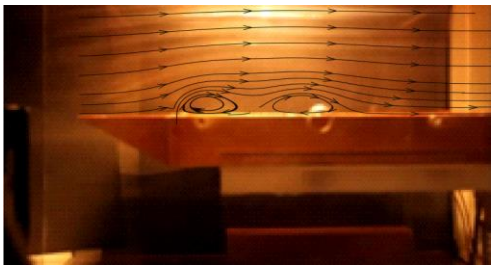

$A_o$=1.4, *Wo*=110, ωt=π/2

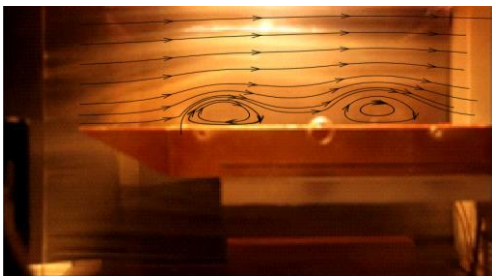

$A_o$=1.05, *Wo*=110, ωt=3π/2

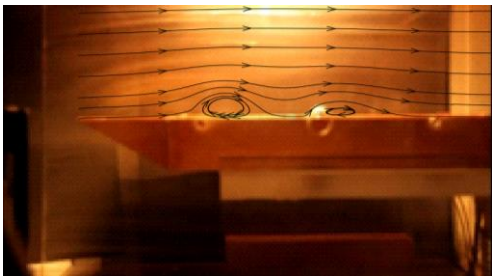

$A_o$=1.4, *Wo*=110, ωt=π

$A_o$=1.4, *Wo*=110, ωt=3π/2

$A_o$=1.4, *Wo*=110, ωt=3π/2

**Fig.7a.** Flow visualization for different amplitude at the fixed frequency and phase angle

**Fig.7b.** Flow visualization over a cycle for the fixed amplitude and frequency

$$Nu_{x,t} = \frac{h(x,t)L}{k} \tag{9}$$

where, $k$ is thermal conductivity of fluid and $h(x,t)$ is the local instantaneous heat transfer coefficient. The overall Nusselt number for the periodic flow can be defined by considering the integration of time and spatial average of the local Nusselt number. Thus, the cycle-averaged Nusselt number is obtained as;

$$Nu_p = \frac{1}{\tau L}\int_{x_o}^{L}\int_{0}^{\tau} Nu(x,t)dtdx \tag{10}$$

where $x_o$ is the heated plate beginning, $\tau$ is the cycle time, and $L$ is the heated plate length. In this case, the cycle-average Nusselt number is obtained as;

$$Nu_p = \frac{q''L}{k(\overline{T}_w - T_\infty)} \tag{11}$$

where, $q''$ is the heat flux from the heater surface, $\overline{T}_w$ is the cycle-averaged heater wall temperature (defined in Eqn(8)), and $T_\infty$ is the average fluid temperature of the forced flow.

The cooling effects of pulsating jet on the plate are investigated by measuring the surface and ambient temperatures for different operating parameters. In this study, the heat transfer performance is defined by an enhancement factor $\eta$ and is given in Eq. (12).

$$\eta = \frac{Nu_p}{Nu_s} \tag{12}$$

where $Nu_p$ is the cycle-averaged Nusselt number (Eqn.11), and $Nu_s$ is the Nusselt number for the steady flow. Thus, a value of $\eta$ over 1.0 denotes the enhanced heat transfer.

In this section, the periodic flow interaction is analyzed between the pulsating jet and forced flow. Preliminary observations showed that compatibility is required to achieve the optimal heat transfer between the forced flow and jet parameter. The optimum interaction of the pulsating jet and forced flow occurs after the critical (Reynolds number) forced flow velocity. When the forced flow velocity is smaller than this critical velocity, the contribution of forced flow on the overall convective heat transfer is lower. Additionally, when the forced flow velocity further increases to this critical velocity, the forced flow in the channel is strong enough to deflect the pulsating jet (Marzouk et al, 2015). Therefore, the forced flow Reynolds number is optimized and starts with $Re$=60000. In this study, the jet mean velocity is kept constant and, the forced flow velocity is changed. Due to the experimental setup limits, the minimum $Re$ number starts with the value of 60000 ($M$=1.35). Four different Reynolds numbers (given through blowing ratios) are considered in the experiments. The effects of pulsating frequency and amplitude are studied for each of the chosen $Re$ number (blowing ratios).

Fig.8 shows the effect of pulsating frequency and amplitude on the averaged Nusselt number at each blowing ratio of $M$=0.5, $M$=0.75, $M$=1 and $M$=1.35. For comparison, the steady flow and continuous jet conditions are shown together with pulsating jet parameters. Fig.8a, shows the effects on heat transfer performance of pulsating jet parameters for the low blowing ratio of $M$=0.5. At a low blowing ratio, the pulsating frequency and amplitude have no effect on the Nusselt number compared with the steady flow and continuous blowing. Furthermore, the heat transfer performance is reduced. Lower blowing ratios cause re-attachment of the jet on the plate surface near the jet exit. For low blowing ratios, the jet does not have a strong lateral momentum along the flow direction, and the jet effect begins to decrease downstream due to reduced coverage. Reducing the blowing ratio causes the jet to adhere closer to the surface. This jet behaviour reduces the time-averaged Nusselt number, and the penetration of jet into the free stream is significantly reduced with a decreasing blowing ratio.

The effect on the Nusselt number of blowing ratio of $M$=0.75 is shown in Fig.8b as a function of pulsating jet parameters. For $M$=0.75, the increase in pulsating frequency and amplitude have little effect with small variations of the Nusselt number. There is a possibility of the jet lift-off that may be affected by pulsations. Thus, a better cooling performance is produced by the pulsating jets.

In Fig.8c and Fig.8d are presented heat transfer enhancement for $M$=1 and $M$=1.35 blowing ratios, respectively. Higher blowing ratios produce stronger jets that tend to lift-off the boundary layer along the plate. As the blowing ratio increases, the lateral momentum of the jet becomes stronger, and a large circulation region occurs around the jet exit. It moves in the flow direction and drifts towards the plate exit. The increasing blowing ratio ($M$) contributes to the enhancement of heat transfer. The influence is more pronounced as the amplitude increases. In addition, higher frequency contributes to the enhancement of heat transfer. At a higher blowing ratio ($M$=1.35) the maximum jet velocity is obtained, and it causes a large-scale vorticity generation in the boundary layer. Thus, the convective heat transfer capacity is enhanced under the conjugate action of a pulsating jet and forced flow.

The flow structure changes in the boundary layer over each pulsation period. This is evident from the flow visualization images in Fig.7. The heat transfer mechanism is expressed in the flow visualization section. The maximum heat transfer improvement was obtained approximately 20% for the high amplitude ($A_o$=1.4) and

high frequency (*Wo*=110) and high blowing ratio (*M*=1.35) compared to the steady flow.

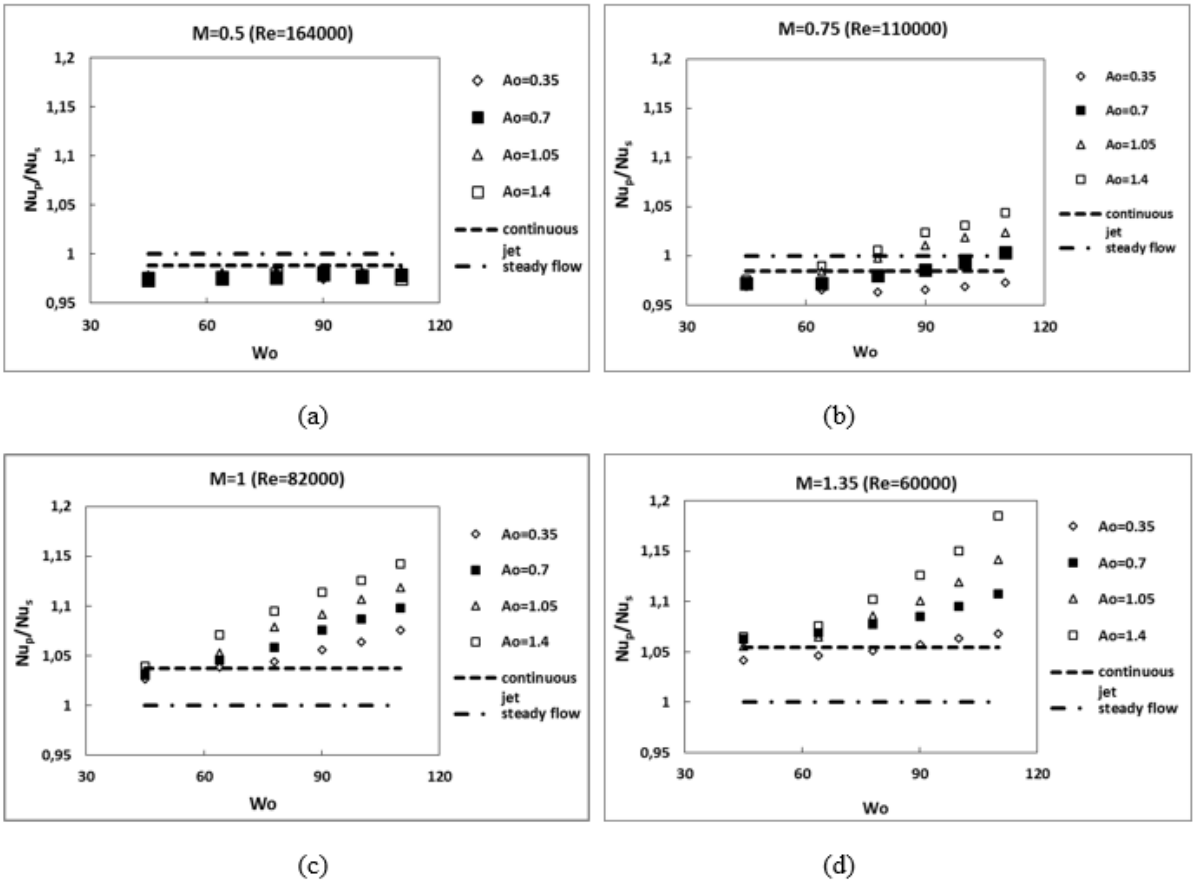


**Fig 8.** Effect of pulsating parameters on the heat transfer performance for different blowing ratios

The results reveal that heat transfer is significantly enhanced by the pulsating jet parameters compared with the steady flow and continuous jet conditions. It is concluded that the pulsating jet actuator increases the heat transfer rate at both the high amplitude and high frequency as well as for the high blowing ratio, as seen in the figures.

## CONCLUSION

This study was performed to investigate the effect of a transversely pulsating jet on surface cooling over a heated flat plate. The following parameters were varied during the study; the frequency and amplitude of the pulsating jet, and jet blowing ratio. The experimental results show that the surface cooling performance is affected by the blowing ratio, jet frequency and jet amplitude. The cooling performance was enhanced at high blowing ratios. Additionally, the heat transfer performance considerably increased with the increasing amplitude and frequency compared with the steady flow and continuous jet blowing. The results show good pulsating jet penetration into the boundary layer that contains a large circulation area on the plate. This causes good mixing between the hot fluid near the plate and the cold fluid in the free flow. The experimental results reveal that there is a disruptive effect of the pulsating jet on the hydrodynamic boundary layer, which improves the surface cooling performance. The present study shows that, the pulsating jet has a strong potential for the heat transfer enhancement of surface cooling of a flat plate.

**Acknowledgements**
The authors gratefully acknowledge the financial support for this study from the Scientific and Technological Research Council of Turkey-TUBITAK (Grant Number: 213M580).

## REFERENCES

Akcay, S., 2015, *Heat transfer enhancement on the flat plate by using pulsating jet*, Master's Thesis, Aksaray University, (in Turkish) Aksaray, Turkey.

Akdag, U., Cetin, O., Demiral, D., and Ozkul, I., 2013, Experimental investigation of convective heat transfer on a flat plate subjected to a transversely synthetic jet. *International Communications in Heat and Mass Transfer*, *49*, 96-103.

Akdag, U., Komur, M. A., and Akcay, S., 2016,. Prediction of heat transfer on a flat plate subjected to a

transversely pulsating jet using artificial neural networks. *Applied Thermal Engineering*, *100*, 412-420.
Akdag, U., Akcay, S., and Demiral, D., 2017, The investigation of the heat transfer characteristics of a cross-flow pulsating jet in a forced flow. *Computational Thermal Sciences, 9(6)*, 567-582.

Audier, P., Fénot, M., Bénard, N., and Moreau, E., 2016, Film cooling effectiveness enhancement using surface dielectric barrier discharge plasma actuator, *International Journal of Heat and Fluid Flow*, Part B, *62*, 247–257.

Coulthard, S. M., Volino, R. J., and Flack, K. A., 2007, Effect of jet pulsing on film cooling—Part I: Effectiveness and flow-field temperature results. *Journal of Turbomachinery*, *129* (2), 232-246.

Dai, S., Xiao, Y., He, L., Jin, T., and Zhao, Z., 2016, Film cooling from a hole with parallel auxiliary holes influences, *Numerical Heat Transfer, Part A: Applications*, *69* (5), 497-511.

Elnady, T., Hassan, I., Kadem, L., and Lucas, T., 2013, Cooling effectiveness of shaped film holes for leading edge. *Experimental Thermal and Fluid Science*, *44*, 649-661.

Engels, G., Peck, R. E., and Kim, Y., 2001, Investigation of a quasi-steady liquid crystal technique for film cooling heat transfer measurements. *Experimental Heat Transfer*, *14* (3), 181-198.

Erkoc, E., Fonte, C. P., Dias, M. M., Lopes, J. C. B., and Santos, R. J., 2016, Numerical study of active mixing over a dynamic flow field in a T-jets mixer—Induction of resonance. *Chemical Engineering Research and Design*, *106*, 74-91.

Heneka, C., Schulz, A., Bauer, H. J., Heselhaus, A., and Crawford, M. E., 2012, Film cooling performance of sharp edged diffuser holes with lateral inclination. *Journal of Turbomachinery*, *134* (4), 041015.

Incropera, F.P., and DeWitt, D.P., 2002, *Fundamentals of Heat and Mass Transfer*, 5th ed., Wiley, New York.

Kanani, H., Shams, M., Ebrahimi, R., and Ahmadian, T., 2008, Numerical simulation of film cooling effectiveness on a flat plate. *International Journal for Numerical Methods in Fluids*, *56* (8), 1329-1336.

Kline, S.J. and McClintock, F.A., 1953, Describing uncertainties in single-sample experiments, *Mech. Eng*., *75* (1),3–8.

Koc, I., Islamoglu, Y. and Akdag, U., 2009, Investigation of film cooling effectiveness and heat transfer coefficient and heat transfer coefficient for rectangular holes with two rows for rectangular holes, *Aircraft Engineering and Aerospace Technology*: An International Journal, *81* (2),106–117.
Lee, J. S., and Jung, I. S., 2002, Effect of bulk flow pulsations on film cooling with compound angle holes. *International Journal of Heat and Mass Transfer*, *45* (1), 113-123.

Lee, K. D., and Kim, K. Y., 2014, Film cooling performance of cylindrical holes embedded in a transverse trench. *Numerical Heat Transfer*, Part A: Applications, *65* (2), 127-143.

Li, G., Zheng, Y., Hu, G., and Zhang, Z., 2013, Experimental investigation on heat transfer enhancement from an inclined heated cylinder with constant heat input power in infrasonic pulsating flows. *Experimental Thermal and Fluid Science*, *49*, 75-85.

Liu, X., Tao, Z., Ding, S., and Xu, G., 2013, Experimental investigation of heat transfer characteristics in a variable cross-sectioned two-pass channel with combined film cooling holes and inclined ribs. *Applied Thermal Engineering*, *50* (1), 1186-1193.

Loudon, C., and Tordesillas, A., 1998, The use of the dimensionless Womersley number to characterize the unsteady nature of internal flow. *Journal of Theoretical Biology*, *191* (1), 63-78.

Marzouk, S., Aissia, H. B., and Le Palec, G., 2015, Numerical study of amplitude and frequency effects upon a pulsating jet. *Computers & Fluids*, *123*, 99-111.

Ramesh, S., Ramirez, D.G., Ekkad, S.V., and Alvin, M.A., 2016, Analysis of film cooling performance of advanced tripod hole geometries with and without manufacturing features, *International Journal of Heat and Mass Transfer*, 94, 9–19.

Rohlf, K., and Tenti, G., 2001, The role of the Womersley number in pulsatile blood flow: a theoretical study of the Casson model. *Journal of Biomechanics*,*34* (1), 141-148.

Schreivogel, P., Abram, C., Fond, B., Straußwald, M., Beyrau, F., and Pfitzner, M., 2016, Simultaneous kHz-rate temperature and velocity field measurements in the flow emanating from angled and trenched film cooling holes, *International Journal of Heat and Mass Transfer*, *103*, 390–400.

Sidik, N. A. C., Kianpour, E., and Golshokouh, I., 2013, Dynamic and Thermodynamic Analysis of Film-Cooling. *International Review of Mechanical Engineering (IREME)*, *7* (3), 570-577.

Singh, K., Premachandran, B. and Ravi, M.R. 2016, Experimental assessment of film cooling performance of short cylindrical holes on a flat surface, *International Journal of Heat and Mass Transfer*, *52* (12), 2849–2862.

Sultan, Q., Lalizel, G., Fénot, M., and Dorignac, E., 2016, Influence of coolant jet pulsation on the convective film cooling of an adiabatic wall, *Journal of Heat Transfer,139* (2), 022201.

Tu, Z., Mao, J., and Han, X., 2017, Numerical study of film cooling over a flat plate with anisotropic thermal conductivity, *Applied Thermal Engineering*, *111*, 968–980.

Wu, H., Cheng, H., Li, Y., Rong, C., and Ding, S., 2016, Effects of side hole position and blowing ratio on sister hole film cooling performance in a flat plate, *Applied Thermal Engineering*, *93*, 718–730.

Xie, G., Zheng , S., and Sundén, B., 2015, Heat transfer and flow characteristics in rib-/deflector-roughened cooling channels with various configuration parameters, *Numerical Heat Transfer*, Part A: Applications , *67* (2), 140-169.

**Selma Akçay,** She was born in 1975 in Kayseri. She completed the Department of Mechanical Engineering at Erciyes University, Turkey, in 2000. She graduated from Aksaray University, Institute of Science and Technology in 2015. She is still a PhD student at Aksaray University. She is working as a Mechanical Engineer at Kayseri Provincial Health Directory. Heat transfer, pulsating flow, computational fluid Dynamics and nanofluids topics are of interest.

**Ünal Akdağ,** He was born in 1970 in Aksaray, He completed the Department of Mechanical Engineering at Erciyes University, Turkey, in 1992. He graduated from Nigde University in 1997 with a Master's degree. He received his PhD in Mechanical Engineering from Istanbul Technical University, in 2005. He was a visiting scholar at Texas A & M University (USA), in 2006. He is working as a Professor at Aksaray University, Mechanical Engineering Department. Heat and mass transfer, oscillating/pulsating flow, computational fluid dynamics, nanofluids and microflow topics are of interest.

**Doğan Demiral,** He was born in 1962 in Sivas. He received his BSc from Erciyes University Mechanical Engineering in 1986 and later on pursued Masters and PhD degrees at the same university Energy Division in 1996. His main research fields are solar energy, convective heat transfer, computational fluid dynamics and nanofluids. He is teaching courses in alternative energy, heat transfer, heat exchanger and fluid mechanics for graduate and undergraduate students.

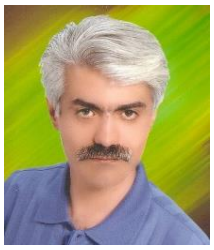

**Hakan Palancıoğlu**, He was born in 1973 in Malatya. He received his BSc from Department of Mechanical Engineering at Firat University, Turkey, in 1999. He graduated from Aksaray University, Institute of Science and Technology in 2011. He is working as a lecturer at from Aksaray University, Mechanical Engineering Department.